

1D simulation of runaway electrons generation in pulsed high-pressure gas discharge

This content has been downloaded from IOPscience. Please scroll down to see the full text.

2015 EPL 112 15001

(<http://iopscience.iop.org/0295-5075/112/1/15001>)

View [the table of contents for this issue](#), or go to the [journal homepage](#) for more

Download details:

IP Address: 143.107.128.59

This content was downloaded on 26/10/2015 at 17:04

Please note that [terms and conditions apply](#).

1D simulation of runaway electrons generation in pulsed high-pressure gas discharge

V. YU. KOZHEVNIKOV, A. V. KOZYREV^(a) and N. S. SEMENIUK

Institute of High Current Electronics - Akademicheskyy ave. 2/3, 634055 Tomsk, Russia and Tomsk State University - Lenin ave. 36, 634050 Tomsk, Russia

received 26 May 2015; accepted in final form 7 October 2015
published online 26 October 2015

PACS 52.80.-s – Physics of plasmas and electric discharges: Electric discharges
PACS 52.65.Ww – Plasma simulation: Hybrid methods

Abstract – The results of theoretical modelling of runaway electron generation in the high-pressure nanosecond pulsed gas discharge are presented. A novel hybrid model of gas discharge has been successfully built. Hydrodynamic and kinetic approaches are used simultaneously to describe the dynamics of different components of low-temperature discharge plasma. To consider motion of ions and low-energy (plasma) electrons the corresponding equations of continuity with drift-diffusion approximation are used. To describe high-energy (runaway) electrons the Boltzmann kinetic equation is included. As a result of the simulation we obtained spatial and temporal distributions of charged particles and electric field in a pulsed discharge. Furthermore, the energy spectra calculated runaway electrons in different cross-sections, particularly, the discharge gap in the anode plane. It is shown that the average energy of fast electrons (in eV) in the anode plane is usually slightly higher than the instantaneous value of the applied voltage to the gap (in V).

Copyright © EPLA, 2015

Introduction. – The phenomenon of runaway electrons generation is of great scientific interest and could be widely applied in science and technology (pumping lasers, excitation of luminescence in crystals, etc.) [1–4].

Recent experimental works [1,2] are worth mentioning. The main characteristics that researchers are eager to know are the runaway electron beam duration, initial and final time points of its formation with respect to the breakdown stage and the beam energy. Due to the complexity of the problem consensus has not yet been reached.

Some numerical simulations are based on methods operating with a restricted ensemble of particles (*i.e.* Monte Carlo methods, PIC methods, etc.) [5,6]. They do not allow to calculate the range of statistically small number of fast electrons. Other authors made successful attempts to simulate runaway electrons in one-dimensional discharge models [7] with a pre-defined mechanism for the initiation of fast electrons as an electron field emission from the cathode surface.

We propose a new approach to a numerical investigation of the runaway electrons problem. First, we assume that the proportion of high-energy electrons is negligible

and they do not affect the discharge dynamics. Then, we describe the dynamics of different components of low-temperature discharge plasma in drift-diffusion approximation. At last, we use the electric field strength distribution and the level of particle generation data to solve the Boltzmann equation for runaway electrons.

Simulation. –

Drift-diffusion approximation of charge particles dynamics in discharge plasma. The electric discharge circuit is made of a connected in-series pulse voltage source $U_0(t)$, a ballast resistor R and a planar discharge gap (spark gap length d , electrode area S) filled with gas at pressure p . To describe in detail the spatial and temporal plasma structure with electric field distribution the following system of continuity equation, equation of conservation of total current density and Poisson's equation was used:

$$\frac{\partial n_e}{\partial t} + \frac{\partial \Gamma_e}{\partial x} = \alpha(E)\mu_e |E| n_e, \quad (1)$$

$$\varepsilon_0 \frac{\partial E}{\partial t} + e(\Gamma_i - \Gamma_e) = j(t), \quad (2)$$

$$n_i = n_e + \frac{\varepsilon_0}{e} \frac{\partial E}{\partial x}. \quad (3)$$

^(a)E-mail: kozyrev@to.hcei.tsc.ru

We used the following expressions for drift-diffusion fluxes:

$$\begin{aligned}\Gamma_e &= -\mu_e n_e E - D_e \frac{\partial n_e}{\partial x}, \\ \Gamma_i &= \mu_i n_i E - D_i \frac{\partial n_i}{\partial x},\end{aligned}\quad (4)$$

and total current density

$$j(t) = \frac{1}{RS} \left\{ U_0(t) - \int_0^d E(x, t) dx \right\}, \quad (5)$$

where n_e , n_i are the electrons and ions densities; μ_e , μ_i the electrons and ions mobility; D_e , D_i the electrons and ions diffusion coefficients; E is the electric field strength; α is the Townsend ionization coefficient

$$\alpha/p = A \exp(-Bp/E); \quad (6)$$

the A, B constants depend on the gas properties; ε_0 is the dielectric permittivity in vacuum and e is the elementary charge.

Boundary conditions for the system (1)–(3) are formulated in terms of border fluxes values. The electrons flux at the cathode is determined by gamma processes intensity, and the ions flux is equal to the drift flux

$$\begin{aligned}\Gamma_e(0, t) &= -\gamma \Gamma_i(0, t), \\ \Gamma_i(0, t) &= \mu_i n_i(0, t) E(0, t),\end{aligned}\quad (7)$$

where γ is the effective coefficient of secondary electron processes at the cathode.

Due to the fact that the drift flux is greater than the diffusion flux, the electron flux to the anode is equal to the drift flux component and the ion flux vanishes, so we obtain

$$\begin{aligned}\Gamma_e(d, t) &= -\mu_e n_e(d, t) E(d, t), \\ \Gamma_i(d, t) &= 0.\end{aligned}\quad (8)$$

The numerical solution of (1)–(3) is based on the specific discretization procedures. The purpose of this method is to reduce the partial differential equations system to the system of ordinary differential equations (method of lines) [8] and to solve them using common ODE solvers (*i.e.* RKF45). As for the fluxes discretization in the continuity equation (1) we apply the WENO-3-LF [9] scheme in the context of the finite-volume method [10] for convective terms.

Boltzmann equation for runaway electrons in discharge.

The flow of runaway electrons in the plasma is formed when the effective decelerating force cannot compensate for the electrostatic force which accelerates the electrons to the anode [11]. This situation is naturally realized for the fast electrons (> 1 keV). Their cross-section of collisions with atoms decreases with the increase of kinetic energy [12]. But fast electrons are almost lack in the initial plasma. They can appear only when statistically unlikely

events occur, *i.e.* when the generated electron does not have time to collide before it can gain a relatively large directed speed. This feature is inherently in the basis for modeling fast electrons kinetics in the discharge.

The main points of the model are formulated as follows: 1) the amount of runaway electrons is small, and we can neglect their influence on the evolution of the gas discharge processes; 2) secondary plasma electrons have Maxwellian distribution function at the time of birth; 3) plasma electrons gain a directed velocity in the previously computed electric field $E(x, t)$, and 4) the first collision of an electron with atoms or molecules leads to the elimination of the runaway electron. In other words, runaway electron dynamics is described as a collisionless transport in the electric field, and any collisions lead to particle loss.

Such behavior is well described by the Boltzmann kinetic equation:

$$\frac{\partial f}{\partial t} + v \frac{\partial f}{\partial x} - \frac{e}{m} E(x, t) \frac{\partial f}{\partial v} = G(x, v, t) - V(f, v). \quad (9)$$

Here, $f(x, v, t)$ is the velocity distribution function of runaway electrons; m is the electron mass. In the right side the rates of generation, G , and disappearance, V , of electrons have the following forms:

$$G(x, v, t) = \left(\frac{\partial n}{\partial t} \right) \cdot \sqrt{\frac{\xi}{\pi}} \exp(-\xi v^2), \quad (10)$$

$$V(f, v) = f(x, v, t) \cdot \nu(v). \quad (11)$$

Here, the generation rate of new electrons matches the right-hand side of eq. (1) (w_e is the electron drift velocity)

$$\left(\frac{\partial n}{\partial t} \right) = \alpha(E) w_e(E) n_e(x, t), \quad (12)$$

but the Maxwell velocity distribution is attached to new electrons initially.

To describe the elimination of fast electrons from the runaway mode, we were guided by the following hypothesis. If during electron acceleration along the field strength vector any scattering collision does not occur, then only this electron can be called “runaway electron”. That is why in expression (11) the frequency of electron collisions has the following model expression:

$$\nu(v) = n_a \sigma^*(v) v = \frac{n_a \sigma_{\max} v}{1 + \eta v^4}. \quad (13)$$

Here, $\sigma^*(v)$ is the velocity dependence transport electron cross-section, σ_{\max} is the low-energy maximum of the transport cross-section, n_a is the concentration of neutral particles. We chose the parameter η such that the transport cross-section, $\sigma^*(v)$, obeyed the well-known asymptotic dependence at high velocity well [12].

The method for solving eq. (9) was based on [13]. The numerical solution was implemented in Mathworks MATLAB.

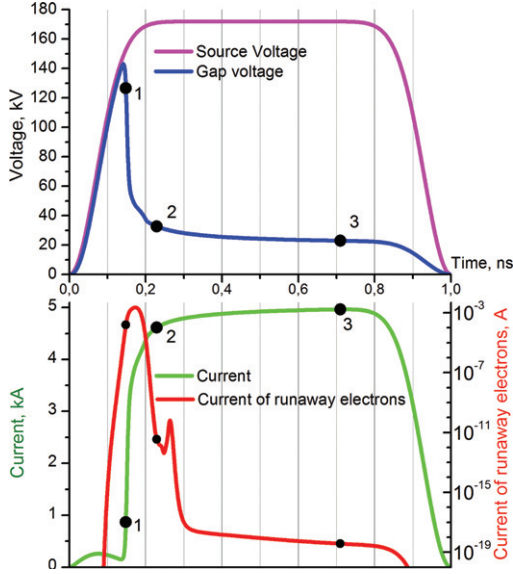


Fig. 1: (Colour on-line) Time dependences of currents and voltages. The three numbered black points correspond to the additional information in figs. 2–5.

Results and discussion. – We investigated nitrogen plasma at atmospheric pressure with homogeneous initial ionization level 10^5 cm^{-3} . The discharge gap was connected in series with the ballast resistor ($R = 30 \Omega$) and voltage source. Its length is $d = 0.5 \text{ cm}$ and the area of the electrodes is $S = 1 \text{ cm}^2$. The pulse of the voltage source has duration of 1 ns with an amplitude of 172 kV. The given pulse amplitude is almost 10 times higher than the static breakdown voltage. Voltage and current pulses waveforms are shown in fig. 1.

We present the numerical parameters attending in the formulas that have been used in the calculations: $\sigma_{\max} = 10^{-17} \text{ cm}^2$, $\gamma = 0.1$, $A = 121 / (\text{cm} \cdot \text{Pa})$, $B = 342 \text{ V} / (\text{cm} \cdot \text{Pa})$, $\mu_e = 382 \text{ cm}^2 / (\text{V} \cdot \text{s})$, $\mu_i = 3.0 \text{ cm}^2 / (\text{V} \cdot \text{s})$, $D_e = 1800 \text{ cm}^2 / \text{s}$, $D_i = 0.046 \text{ cm}^2 / \text{s}$. Diffusion coefficient and electron mobility according to Einstein’s relation formally correspond to an electron temperature of 4.7 eV. Therefore, in (10), the coefficient ξ is selected so that secondary electrons have a similar initial temperature (namely, it was taken into account 5 eV).

Discharge spatial structure evolution. At the first stage of the discharge (less 0.14 ns) gas ionization is uniform over the entire gap excepts for the narrow cathode region whose width increases and reaches approximately $8 \cdot 10^{-3} \text{ cm}$ by the end of this stage. The field strength in the cathode region slightly increases, and the voltage across the gap reaches its maximum value, 143 kV.

Further discharge evolution is accompanied by a sharp gap voltage decline and by the discharge current increase. At this time point, 0.15 ns (number 1 in fig. 1), the gas breakdown profile corresponds to the picture shown in fig. 2. The space of discharge can be distinguished into two zones: i) the cathode region of the enhanced field strength and ii) the quasi-neutral plasma discharge column. The

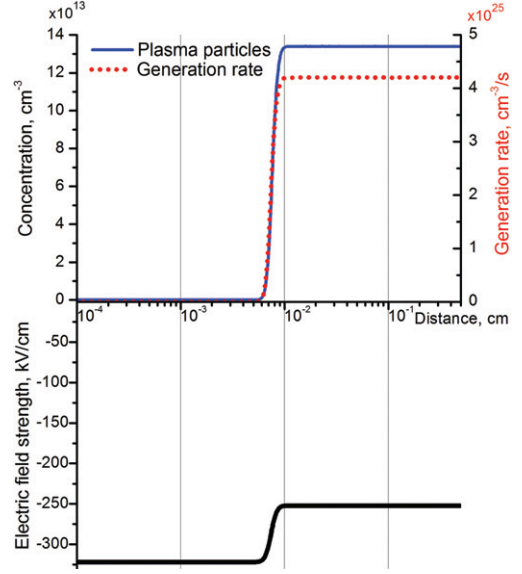


Fig. 2: (Colour on-line) Spatial distributions of the electric field strength, plasma particles concentration, and the ionization rate at the time point of 0.15 ns. The instant source voltage is $U_0 = 153 \text{ kV}$, the voltage at the gap is $U = 126 \text{ kV}$, the current is $I = 0.87 \text{ kA}$.

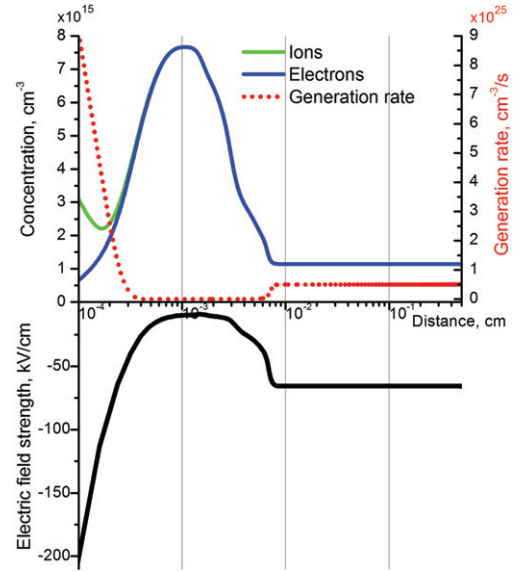


Fig. 3: (Colour on-line) Spatial distributions of the electric field strength, plasma particles concentration, and the ionization rate at the time point of 0.23 ns. The instant source voltage is $U_0 = 171 \text{ kV}$, the voltage at the gap is $U = 33 \text{ kV}$, the current is $I = 4.61 \text{ kA}$.

field strength at the cathode is maximum and about 30% more than in the column. Despite this redistribution of the field, the main ionization is still going in the discharge column (ii), because in the cathode region (i) electron concentration has a very low level.

The next stage of the breakdown is the formation of the intermediate discharge structure, which is shown in fig. 3

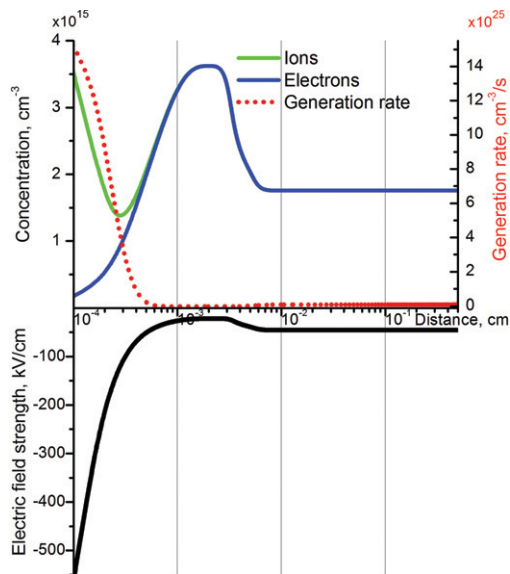


Fig. 4: (Colour on-line) Spatial distributions of the electric field strength, plasma particles concentration, and the ionization rate at the time point of 0.71 ns. The instant source voltage is $U_0 = 172$ kV, the voltage at the gap is $U = 23$ kV, the current is $I = 4.96$ kA.

(the time point corresponds to point 2 in fig. 1). It should be noted that there are two clearly defined ionization fields of the gas separated by a layer where the gas ionization practically stops. Moreover, the generation rate of electrons in the cathode region significantly exceeds the rate of generation of electrons in the discharge column.

Eventually the electric field in the discharge column falls off and the well-known structure of the stationary glow discharge is formed [14,15]. This stage takes place at the end of the applied voltage pulse, and the picture shown in fig. 4 corresponds to the third point in fig. 1. At this stage gas ionization occurs primarily in the cathode layer of the enhanced field.

Generation of runaway electrons. The spatial distribution of the electric field $E(x, t)$ calculated in the discharge simulation was used for the numerical integration of the Boltzmann equation (9) for the velocity distribution function of the runaway electron $f(x, v, t)$.

As well as in our formulation runaway electrons are the electrons that do not collide, in each section (including the anode plane) we have a wide range of energy, most of which contained the plasma electrons with low energy. Of course, we are interested only in fast electrons, *i.e.* those usually observed by the experimenters [1–5]. Therefore, in order to calculate a fast electrons spectrum at the anode we added a foil filter that cuts off the low energetic part (<10 keV) of the electron beam. The attenuation factor of the filter corresponds to a thickness of the aluminum foil of $10 \mu\text{m}$ [16]. The current pulse of runaway electrons at the anode after the aluminum filter is shown in a logarithmic scale in the bottom graph of fig. 1.

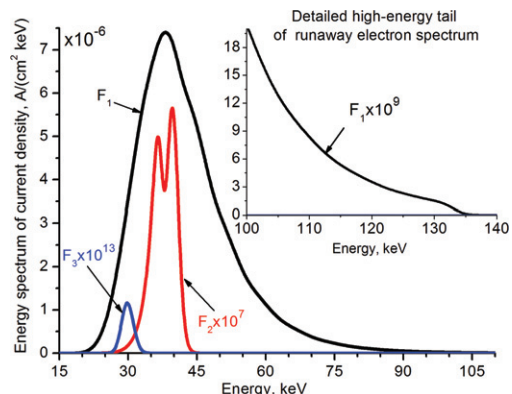


Fig. 5: (Colour on-line) Runaway electron energy distribution function after passing through $10 \mu\text{m}$ aluminium foil at different time points: F_1 at 0.148 ns, F_2 at 0.236 ns, F_3 at 0.710 ns. The instantaneous voltage at the gap is 123 kV, 32 kV and 23 kV, respectively.

Let us discuss on the runaway electrons flux energy spectrum after passing through the foil at certain time points marked by the black points in fig. 1.

The fast electrons energy spectrum for the first selected time (0.15 ns) is shown in fig. 5 as line F_1 . It has a maximum at 39 keV and a long “tail” of the distribution function, which extends up to 135 keV (as it is shown in the right top corner subplot). This spectrum shape is due to the fact that the area of electrons generation is located only in the discharge column and occupies almost the entire gap, as shown in fig. 2. Some excess of electrons maximum energy of the spectrum compared to the instantaneous value of the anode voltage is explained by the finite time motion of electrons from the cathode to the anode when the anode voltage reached its maximum of 143 kV.

Although at later times (points 2 and 3 in fig. 1), there is practically no fast electrons, our method allow to calculate a spectrum and explain the reasons of its transformation. Figure 5 shows filtered spectra for all discharge stages.

At time point 0.236 ns (point 2 in fig. 1, and discharge structure in fig. 3) discharge has two spatially separated electrons generation regions, as shown in fig. 3. As expected, this leads to a two-peak shape of the energy spectrum of runaway electrons that are shown in fig. 5 as line F_2 . The first peak corresponds to electrons generated in the discharge column; the second peak was created by electrons of the near-cathode region. During the discharge evolution the first peak of the distribution function progressively decreases and vanishes. The second peak is shifted to lower energies due to the voltage decrease across the gap, and it decreases in amplitude under the influence of two factors: the increasing average cross-section of the electron-atom collision and the decreasing probability of electrons passing through the foil.

Since the voltage across the gap continues to decrease, the most energy of fast electrons at the anode is always higher than the instantaneous value of $qU(t)$.

Conclusion. – A numerical hybrid model for one-dimensional non-stationary gas discharge with drift-diffusion approximation for electrons dynamics and collisionless transport of runaway electrons is presented. The peculiarity of the mathematical model is the use of the equation of conservation of the total current density to calculate the electric field evolution. Poisson’s equation was used to calculate the spatial ions distribution. A new approach in the calculation is the joint solution of the kinetic Boltzmann equation for runaway electrons with transport equations for plasma particles.

It should be noted that our model deals only with a transverse uniform field which was spatially non-uniform in all experiments (the electric field is essentially three dimensional). In the experiments, the electric field strength in strong geometrical distortion is several times greater than the average value (U/d). Therefore, we did not expect a literal match of our theoretical predictions with certain experimental data. A one-dimensional model is designed to perform other tasks: to determine the principal place of runaway electrons initiation, and to investigate the possible energy spectrum.

As an example, some interesting details result from the appearance of a second small peak of runaway electrons current near the end of the switching stage, as shown in fig. 1. It appears due to the “belated” runaway electrons generated at the current maximum. At this point, the gap voltage is about 30 kV. At this voltage the estimated flight time for the electron from the cathode to the anode is just 100 ps; this corresponds to a delay of the second peak with respect to the main one.

Our model allows to investigate the breakdown and the formation of quasi-stationary discharge forms. One can plot the concentrations of charged particles, electrons, and the rate of generation of the electric field. The solution of the Boltzmann equation gives a dynamic picture of collisionless electrons energy spectra. Similar distribution functions have been obtained previously by other researchers using the Monte Carlo method [17]; they are in a good agreement with our results. The main advantage of the introduced model compared to “particles methods” is that it allows one to calculate an energy spectrum even for a negligible small fast electrons flow. This can be of great interest to the corpuscular diagnostics of plasma processes [18].

It should be noted also that when the gap voltage falls the electrons with energies above the instantaneous value of $qU(t)$ are observed.

This work is supported by the Russian Fund of Basic Research (projects 15-08-03983 and 15-58-53031).

REFERENCES

- [1] CHENG ZHANG, TARASENKO V. F., TAO SHAO, BELOPLOTOV D. V., LOMAEV M. I., SOROKIN D. A. and PING YAN, *Laser Part. Beams*, **32** (2014) 331.
- [2] TAO SHAO, CHENG ZHANG, ZHENG NIU, PING YAN, TARASENKO V. F., BAKSHT E. K., BURACHENKO A. G. and SHUT’KO YU. V., *Appl. Phys. Lett.*, **98** (2011) 021503.
- [3] MESYATS G. A., YALANDIN M. I., REUTOVA A. G., SHARYPOV K. A., SHPAK V. G. and SHUNAILOV S. A., *Plasma Phys. Rep.*, **38** (2012) 29.
- [4] SMIRNOV B. M. and TERESHONOK D. V., *EPL*, **107** (2014) 55001.
- [5] BAKSHT E. K., BELOMYTTSEV S. Y., BURACHENKO A. G., RYZHOV V. V., TARASENKO V. F. and SHKLYAEV V. A., *Tech. Phys.*, **57** (2012) 998.
- [6] KUTSYK I. M., BABICH L. P., DONSKOI E. N. and BOCHKOV E. I., *Plasma Phys. Rep.*, **38** (2012) 891.
- [7] BABICH L. P. and KUTSYK I. M., *High Temp.*, **33** (1995) 190.
- [8] SCHIESSER W. E., *A Compendium of Partial Differential Equation Models. Method of Lines Analysis with Matlab* (Cambridge University Press, New York) 2009.
- [9] XU-DONG LIU, OSHER S. and CHAN T., *J. Comput. Phys.*, **115** (1994) 200.
- [10] VERSTEEG H. K. and MALALASEKERA W., *An Introduction to Computational Fluid Dynamics. The Finite Volume Method* (Longman Scientific & Technical, New York) 1995.
- [11] DREICER H., *Phys. Rev.*, **115** (1959) 238.
- [12] BETHE Y. A., *Ann. Phys. (Berlin)*, **5** (1930) 325.
- [13] XIONG T., QIU J.-M., XU Z. and CHRISTLIEB A., *J. Comput. Phys.*, **273** (2014) 618.
- [14] KOZHEVNIKOV V. YU., KOZYREV A. V. and KOROLEV YU. D., *Plasma Phys. Rep.*, **32** (2006) 949.
- [15] RAIZER YU., *Gas Discharge Physics* (Springer-Verlag, Berlin) 1991.
- [16] TABATA N. and ITO R., *Nucl. Instrum. Methods*, **127** (1975) 429.
- [17] BOICHENKO A. M., TKACHEV A. N., BURACHENKO A. G., KOSTYRYA I. D. and TARASENKO V. F., *Tech. Phys.*, **56** (2011) 1202.
- [18] TAO SHAO, WENJIN YANG, CHENG ZHANG, ZHI FANG, YIXIAO ZHOU and SCHAMILOGLU E., *EPL*, **107** (2014) 65004.